Cavendish–HEP–97/03
July 1997
Revised October 1997

Top-antitop pair production via b-quark initiated processes at the Large Hadron Collider

Stefano Moretti[1]

Cavendish Laboratory, University of Cambridge, Madingley Road, Cambridge, CB3 0HE, United Kingdom.

Abstract

We study $bt\bar{t}$ production via subprocesses initiated by b-quarks at the Large Hadron Collider. Both QCD and electroweak interactions are included in the elementary scattering amplitudes for $bg \to bt\bar{t}$. Since the additional jet in the final state (arising from the bottom quark) is in most cases at very low transverse momentum and very high pseudorapidity, it tends to escape detection. Therefore, such a process can act as a background to double-top as well as to single-top channels exploited in top quark phenomenology at present and future hadron colliders. Furthermore, if the additional b-jet can be tagged then $bt\bar{t}$ samples can be exploited in constraining possible effects of New Physics. The relevance of this reaction in such contexts is discussed and various total and differential rates of phenomenological interest are given.

[1]E-mail: moretti@hep.phy.cam.ac.uk

1. Introduction

The main production channel of top quarks at hadron colliders is that proceeding through $q\bar{q}$ and gg partonic scatterings [1], that is, via

$$q\bar{q} \to t\bar{t}, \tag{1}$$

and

$$gg \to t\bar{t}, \tag{2}$$

mediated by QCD, being the electroweak (EW) contributions $q\bar{q} \to \gamma^*, Z \to t\bar{t}$ much smaller[2].

This mode has been exploited in the recent discovery of the top quark at the Tevatron [2]. The latest value of the top mass as measured from the the CDF and D0 experiments is $m_t = 175.6 \pm 5.5$ GeV [3], which is in very good agreement with that derived within the Standard Model (SM) from EW measurements at LEP, SLC, SPS, Tevatron and in neutrino scattering experiments [4]: $m_t = 177 \pm 7^{+16}_{-19}$ GeV. This clearly represents a great success of the theory. Furthermore, it is worth recalling that when the mass of the $W^\pm$ boson will be determined to a precision of 50 MeV or less (at LEP 2), the EW theory will also significantly reduce the allowed range for the mass of the Higgs boson.

It is clear that the discovery of the top quark and the measurement of its mass are only the first steps. In the near future, various details of the production process as well as of the decay channels will have to be thoroughly studied and other fundamental top parameters (the width, the couplings, etc.) will have to be determined. In this respect, a second mode that will be studied at the Tevatron is the production channel involving one top quark only [5]. Although the first mechanism (i.e., double-top production) is dominant both at the Tevatron and the Large Hadron Collider (LHC) [6], the second (i.e., single-top production) is very well suited for studying the coupling between the $W^\pm$ boson and the top and bottom quarks [7]. In fact, the measurement of the Cabibbo-Kobayashi-Maskawa (CKM) matrix element V_{tb} cannot be easily performed via $t\bar{t}$-production and decay. On the one hand, top-antitop pairs are produced through a 'flavour blind' $gt\bar{t}$ vertex. On the other hand, the dependence on V_{tb} entering in the width of the top is 'canceled' by the fact that branching fraction for the decay $t \to bW^\pm$ is close to one in the SM, which predicts $0.9989 \leq |V_{tb}| \leq 0.9993$ at the 90% confidence level [8]. In the end, in $t\bar{t}$ samples, one can establish a lower limit on $|V_{tb}|$ by studying the polar angle of the lepton produced in the top decay channel $t \to bW^\pm \to b\ell\nu_\ell$. In contrast, the single-top production rates are directly proportional to $|V_{tb}|^2$, so that a simple measurement of total cross section can lead to a high precision determination of the CKM matrix element describing the mixing between top and down-type quarks.

The variety of mechanisms which produce only one top in the final state is very rich. They all involve EW interactions. They can be conveniently grouped according to the final state produced and to the virtual particle content (see Ref. [9]), as

$$tb - \text{production} \qquad pp, p\bar{p} \to t\bar{b}X \qquad (\text{via } s\text{-channel } W^{\pm *}\text{-bosons}), \tag{3}$$

$$tq - \text{production} \qquad pp, p\bar{p} \to tqX \qquad (\text{via } t, u\text{-channel } W^{\pm *}\text{-bosons}), \tag{4}$$

[2]They amount to $\approx 8\%$ of the total cross section both at the Tevatron and the Large Hadron Collider (see later on).

$$tW^{\pm} - \text{production} \qquad pp, p\bar{p} \to tW^{\pm}X \qquad (\text{via } s[t,u]\text{-channel } b[t]^{*} \text{ quarks}), \tag{5}$$

where q represents a light (anti)quark, b and t a bottom and a top (anti)quark, respectively.

Although the event rate of single-top production at the Tevatron is at present rather small[3], this mode will soon be investigated intensively. In fact, by 1999 the new Main Injector at the Tevatron should be operating, boosting the centre-of-mass (CM) energy $\sqrt{s}_{p\bar{p}}$ of the colliding proton-antiproton beams from 1.8 TeV of the so-called 'Run 1' (during the past years 1992–1996) to 2 TeV for the forthcoming 'Run 2' (1999–2001). An increase of the total peak luminosity is also foreseen, by one order of magnitude, up to $L = 2 \times 10^{32}$ cm^{-2} s^{-1}. A final stage of the Tevatron has also been proposed: the 'Run 3', always at $\sqrt{s}_{p\bar{p}} = 2$ TeV but with the increased luminosity $L = 10^{33}$ cm^{-2} s^{-1} (thus denominated 'TeV33', planned for the years 2003–2006). Eventually, the pp accelerator LHC at CERN will take over, starting operations in 2005, with a CM energy of 14 TeV and a peak luminosity in the range $10^{32} - 10^{33}$ cm^{-2} s^{-1} (Run 1).

The processes (1)–(5) represent the most frequent production modes of top quarks at the hadronic colliders of the present and future generation and they have been extensively studied in the literature. Many of their higher order corrections have also been calculated (mainly from QCD) and incorporated in the experimental Monte Carlo programs [10]. It should however be noticed that the accuracy of the experimental measurements is continuously increasing and the huge amount of data which will be collected over the next decade will seriously challenge the current reliability of the perturbative predictions, so that further theoretical efforts will soon be needed in order to match the advances on the experimental side. In this respect, it is clear that the increase in luminosity and in CM energy available will for example mean that rarer production channels of top quarks could yield detectable rates at the new generation of hadronic machines.

It is the purpose of this letter to study the production of top-antitop pairs via b-quark initiated processes, through the two-to-three body reaction

$$bg \to bt\bar{t}, \tag{6}$$

at both the Tevatron and the LHC. The Feynman diagrams describing this process are given in Fig. 1a–b. In our opinion, there are at least three good reasons to expect that these events can eventually become interesting in top physics.

1. Although the final state of reaction (6) always involves an additional jet with respect to that produced via processes (1)–(2), this tends to be at very low transverse momentum and very large pseudorapidity. Therefore, in most cases, it escapes detection and the final signature is precisely that of top-antitop production and decay (1)–(2).

2. As the typical (partonic) energy available at supercolliders increases, the content of b-quarks inside the colliding protons is very much enhanced [11], this yielding a much higher probability for b-quark initiated scatterings to take place.

3. Contrary to the case of the $t\bar{t}$ channel, for which EW contributions are due to only two additional diagrams, for reaction (6) the number of EW diagrams is much larger than that of the QCD ones (compare Fig. 1a against Fig. 1b), this rendering the EW contributions important in the total cross section.

[3] For a review of typical single-top cross sections, see, e.g., Refs. [6, 9].

The impact of even small corrections to $t\bar{t}$ production and decay via $q\bar{q}$- (dominant at the Tevatron) and gg- (dominant at the LHC) scatterings could be crucial both in studying SM effects and from the point of view of the searches for New Physics. In the first case, $bt\bar{t}$ events are interesting as they can represent a background to radiative top decays [12], such as $t\bar{t}(g) \to b\bar{b}W^+W^-g$ (which constitute a testing ground of QCD), as well as to three-body top decays, such as $t \to bW^\pm Z$ and especially $t \to bW^\pm H$ [13] (in which $Z, H \to b\bar{b}$). In the second case, one should recall that, being the mass of the top of the order of the EW symmetry breaking scale (the vacuum expectation value is in fact 246 GeV), top phenomenology represents one of the most promising places where to search for phenomena beyond the realm of the SM [14]. Therefore, to assess exactly the amount of all sizable corrections within the ordinary dynamics is a benchmark task to be achieved in order to establish possible deviations from the standard theory.

Among the various possible effects of New Physics which could be investigated in (both single- and double-) top studies at hadron colliders [15]–[21], we discuss here only two, which are relevant to the case of $bt\bar{t}$ phenomenology. First, various models for dynamical EW symmetry breaking [15] predict the existence of heavy colour-singlet and colour-octet vector states strongly coupled to the top quark, the so-called 'colorons' [16]. These could produce a resonance decaying into $t\bar{t}$-pairs. Therefore, the effects of the new particles should be visible in the spectrum of the $t\bar{t}$ invariant mass. Second, if there are more than six quarks, the CKM matrix element $|V_{tb}|$ could be anywhere between (almost) zero and unity, depending on the amount of mixing between the third and fourth generation, whereas non-universal top couplings differing from the SM form $V - A$ should appear as a deviation from the branching ratio of top quarks into $bW^\pm$-pairs with the gauge bosons polarised longitudinally (which happens around 69% of the times in the SM). By studying the angular distributions of the charged lepton in $t\bar{t}$-decays [22], one can extract limits on the form of the $W^\pm tb$ coupling.

A very last motivation that we put forward to justify our analysis is based on the observation that the three-vertex process (6) possibly involves large (compared to the QCD ones, see point 3. above) contributions with two EW couplings. In some instances these are both $W^\pm tb$ vertices (graphs 1, 5, 9 and 13 in Fig. 1b), so that $|V_{tb}|^4$ terms enter in the total cross section of reaction (6). Indeed, we will show that diagram 5 in Fig. 1b is the dominant EW contribution, as all the other diagrams in Fig. 1b amount to only $\approx 2\%$ of the EW part[4]. Therefore, provided the EW contribution is large enough in the total cross section (and the QCD one is subtracted), rates from process (6) will show a high sensitivity to variations of $|V_{tb}|$. More in general, all the couplings of the EW model involving a top-quark appear in the diagrams of Fig. 1b. Therefore, a large variety of possible deviations from the SM dynamics could be tested in $bt\bar{t}$ events: in particular, the existence of a fourth generation of quarks (u_4, d_4) with a down-like quark d_4 with mass around 175 GeV. In fact, the new particle would reveal itself 'directly' in the $\gamma d_4\bar{d}_4$ and $Zd_4\bar{d}_4$ vertices of the theory. More important, when a d_4 flavour is produced instead of a top via process (6), diagrams 1, 5, 9 and 13 of Fig. 1b do not appear any longer, so that the total cross section should suffer from a large depletion. In contrast, in single-top studies via measurements of the $|V_{tb}|$ matrix element the effects of new flavours could pass

[4]Note that, for reason of gauge invariance, also diagram 1 must be included together with diagram 5 in the computation, although this is very much suppressed because of the $g \to t\bar{t}$ splitting. In addition, graphs 9 and 13 are negligible, because of the splitting into tb-pairs of a real $W^\pm$.

unobserved, in case of an extremely small mixing of the third and fourth generation. It will be one of our main concerns to quantify the relevance of the diagrams in Fig. 1b with respect to those in Fig. 1a, which only involve gluon-fermion-antifermion vertices, so that their contribution is insensitive to the flavour. This can also be affirmed for pair production of d_4-quarks from $q\bar{q}$ and gg-fusion, the counterpart of processes (1)–(2).

In summary, the final aim of our study is to assess the relevance of $bt\bar{t}$ events as background in both double- and single-top phenomenology as well as their own importance in 'confirming the identity' of the particle recently discovered at Fermilab. The material we will present has been organised as follows. In the next Section we give some details of the calculation and list the values adopted for the various parameters. Section 3 is devoted to a discussion of the results. The conclusions are in Section 4.

2. Calculation

The tree-level Feynman diagrams that one needs for computing process (6) are given in Fig. 1a–b. The pure QCD graphs are displayed in Fig. 1a whereas those involving also EW vertices are given in Fig. 1b. To calculate the corresponding amplitudes squared we have used MadGraph [23] and HELAS [24]. The codes produced have been carefully checked for gauge and BRS [25] invariance. The integrations over the appropriate phase spaces have been performed using VEGAS [26][5].

The b-quark in the initial state of reaction (6) has been treated as a constituent of the proton with the appropriate momentum fraction distribution $f_{b/p}(x, Q^2)$, as given by the partonic structure functions. So has been done for the gluon. However, as the parton distribution functions (PDFs) of b-quarks inside the proton suffer from potentially large (theoretical) uncertainties[6] (see, e.g., Ref. [11]) and those of the gluon are not so well known at small x, we have produced our results in the case of several different recent next-to-leading structure functions, such as the sets MRRS(1,2,3) [31] and CTEQ4(HQ) [34], which give excellent fits to a wide range of deep inelastic scattering data (including the measurements from the HERA ep collider) and to data on other hard scattering processes. In each case the appropriate value of $\Lambda^{(n_f)}_{\overline{MS}}$ (in the modified Minimal-Subtraction scheme) has been used. The QCD strong coupling α_s entering explicitly in the production cross sections and implicitly in the parton distributions has been evaluated at two-loop order, with $\Lambda^{(n_f\neq 4)}_{\overline{MS}}$ calculated according to the prescriptions in Ref. [35] and (in general) at the scale $\mu = \sqrt{\hat{s}}$ (i.e., the CM energy at partonic level). However, since the choice of the scale for the structure functions and for α_s represents a source of uncertainty, we have studied the yields of process (6) also in case of other representative values of μ.

In the numerical calculations presented in the next Section we have adopted the following values for the electromagnetic coupling constant and the weak mixing angle: $\alpha_{em} = 1/128$ and $\sin^2\theta_W = 0.2320$. For the gauge boson masses and widths we have taken

[5]Note that in computing the rates for process (6) we also have included the contribution due to the charged conjugated diagrams of Fig. 1a–b (i.e., those proceeding via $\bar{b}g$-fusion).

[6]In fact, the b-sea distributions are not measured by experiment, rather these are obtained from the gluon distributions splitting into $b\bar{b}$ pairs by using the Dokshitzer-Gribov-Lipatov-Altarelli-Parisi evolution equations [27] and, in general, the implementation of such dynamics is very different from set to set in those currently available on the market [28]–[34].

$M_Z = 91.19$ GeV, $\Gamma_Z = 2.5$ GeV, $M_{W^\pm} = 80.23$ GeV and $\Gamma_{W^\pm} = 2.08$ GeV, while for the fermion masses we have used, in general, $m_b = 4.3$ GeV (to match the value used in the MRRS(1,2,3) PDFs) and $m_t = 175$ GeV [3]. We have changed the value of m_b into 5 GeV when using the CTEQ4(HQ) PDFs and adopted the additional values 165, 170, 180 and 185 GeV for m_t when studying the effects of a possible fourth generation of quarks. For simplicity, we have set the CKM matrix element of the top-bottom coupling equal to one.

The Higgs boson of the SM enters directly in the diagrams of Fig. 1b. As default value for its mass we have used $M_H = 150$ GeV, according to the best χ^2 fit as obtained from the analysis of the LEP and SLC high precision EW data: i.e., $M_H = 149^{+148}_{-82}$ GeV [4]. However, since the constraints on the Higgs mass are rather weak (a lower bound of 66 GeV from direct searches [36] and a 95% confidence level upper limit of 550 GeV from the mentioned data exist [37]) we have studied the M_H dependence of the EW contributions of process (6).

Finally, as total CM energies of the colliding beams at the Tevatron and the LHC we have adopted the values $\sqrt{s}_{p\bar{p}} = 2$ and $\sqrt{s}_{pp} = 14$ TeV, respectively.

3. Results

As a first result we quote the cross section for events of the type (6) at $\sqrt{s}_{p\bar{p}} = 2$ TeV. This is very very small, around 2–3 fb. Thus, it is negligible both in double-top and single-top phenomenology. In fact, at lowest order, the total cross section of the former is around 8 pb [6] whereas that of the latter is approximately 3 pb [6, 9]. That is, process (6) represents a correction of the order of one part in ten thousands. In fact, rates become even smaller when acceptance cuts (in transverse momentum, pseudorapidity and separation of the detectable particles) are implemented, in all possible top-antitop decay channels: hadronic, semi-hadronic(leptonic) and purely leptonic as well. The number of produced events is in itself tiny too, a few tens at the most at only during Run 3. Clearly, this is of no experimental relevance. In contrast, at the LHC, the total cross section is more than three orders of magnitude larger. Therefore, in the following we will focus our attention to the case of the CERN hadron collider only.

Before presenting our results for the LHC a few words are needed concerning the dynamics of process (6). In particular, we would like to point out that its cross section is finite over all the available phase space (when all masses are retained in the calculation). This allow us to safely calculate the rates of process (6) in both the following cases: (i) when the additional b-quark in the final state is produced in the detector acceptance region and (ii) when it escapes detection either because at low transverse momentum or because at large pseudorapidity. Indeed, from the point of view of top-antitop phenomenology the latter case is more interesting. In fact, as mentioned in the Introduction, a reason to study reaction (6) is that it represents an irreducible contribution to top-antitop production and decay when the additional jet goes undetected. The former case is instead interesting as it can represent a background to radiative top decays and to three-body top decays.

Furthermore, we should also mention that in calculating the differential distributions involving the top decay products we have in general resorted to a Narrow Width Approximation (NWA), as we have written the heavy quark propagator as

$$\frac{\not{p} + m_t}{p^2 - m_t^2 + i m_t \Gamma} \left(\frac{\Gamma}{\Gamma_t}\right)^{\frac{1}{2}}, \tag{7}$$

where Γ_t is the tree-level top width and where the numerical value adopted for Γ has been 10^{-6}. This way, one is able to correctly reproduce the rates for $t\bar{t}X$ production times the (squared) branching ratio $[BR(t \to bW^{\pm})]^2$, as it is done in many of the experimental simulations, which indeed do not include finite width effects [38]. Incidentally, this simplifies considerably the numerical calculations as one can integrated out the Breit-Wigner dependence of the two top quarks, thus reducing by two the number of variables of the multidimensional integrations. (We have verified that the spectra of quantities involving the b's, the leptons and the light jet produced in the top decays suffer little from NWA effects.) The only exception has been made when plotting the distribution in the partonic CM energy, for which the exact results have been obtained (i.e., $\Gamma \equiv \Gamma_t$).

Finally, we identify the jets in the final state with the partons from which they originate, we introduce no jet energy smearing and apply all cuts at parton level.

3.1 Theoretical error

The rates of process (6) depend strongly on the b-quark parton distribution function inside the proton. On the one hand, such density is very poorly constrained by the data, as even the extreme case in which this is neglected the derived parton densities (such as the GRV PDFs [39, 40]) can adequately fit the available data. On the other hand, there has been a lot of theoretical activity in the recent years in the field of heavy quark distributions (although mainly focused to the case of charm quarks) [31, 34, 41, 42]. In the latter context, it should be mentioned that two approaches had dominated the literature in the past years: the so-called TFN-scheme, where TFN stands for *Three-Flavour-Number* (such as in the GRV sets), and the FFN-scheme, where FFN stands for *Four(and Five)-Flavour-Number* (such as in the MRS and CTEQ parton densities). In the first case, only the 'light' flavours $\{g, u, d, s\}$ participate in the parton dynamics inside the proton, and heavy flavours can only be created in scattering processes (i.e., 'flavour creation'). In the second case, also the 'heavy' quarks $\{c, b, (t)\}$ are numbered among the initial state partons, provided the energy scale of the interaction is large enough (though in most cases the 'massive' parton are indeed treated as 'massless', once the density is turned on at the appropriate threshold[7]), so that heavy quarks in the final state can also be obtained by exciting the corresponding flavour inside the proton (i.e., 'flavour excitation'). It turns out that (see, e.g., Refs. [42]) the TFN-scheme is the most suitable for the heavy quark component of the PDFs near threshold whereas well above this regime is the FFN-scheme that should be used.

More recently, a consistent formulation of heavy flavour dynamics within the perturbative-QCD (pQCD) framework has been given, in Refs. [31, 41, 42]. The new treatment encompasses both the 'flavour creation' and 'flavour excitation' mechanisms and is valid from the heavy quark threshold up to the high energy regime. It reduces to the two above approaches in the appropriate limits: i.e., to the TFN scenario when

[7]For a comparison between mass-dependent and mass-independent evolution of PDFs, see Ref. [11].

$\mu \sim m_q$ and to the FFN one if $\mu \gg m_q$ (where $q = c, b$)[8]. Although the three formulations in Refs. [31, 41, 42] are slightly different, their approach is basically the same. Furthermore, based on the improved theory for heavy quark dynamics, global analyses and new PDF packages have been made available, such as the MRRS(1,2,3) [31] and CTEQ4(HQ) [34] sets.

Preliminary comparisons between the various 'heavy quark sets' have been performed in Refs. [41, 42, 43], though results are not conclusive yet, since similarly fitted parton distributions in the various schemes are not available in the literature at the moment, to allow for a consistent study [34]. Being such a comparison beyond the scope of this paper, we confine ourselves to the computation of some relevant rates of process (6) with the four new sets of parton distributions. The total cross section for $bg \to bt\bar{t}$, before any acceptance cut, is given in Tab. I for MRRS(1,2,3) and CTEQ4(HQ), at the LHC. Indeed, Tab. I shows that the differences among the four sets of PDFs are reasonably contained. In fact, if one assumes as default the MRRS(3) value, the largest difference occurs with respect to CTEQ4(HQ) one, about +10%. Rather than an absolute value, such a difference should be considered as a *lower limit* (for the present time) on the error affecting the rates of process (6) due to the PDFs.

Before proceeding further, it should be noticed that, together with process (6), one should also consider another reaction, namely

$$gg \to b\bar{b}t\bar{t} \qquad \text{(via } g \to b\bar{b} \text{ splitting)}, \tag{8}$$

which gives the same final state as the process $bg \to bt\bar{t}$ if one of the b-jets is close enough to the beam pipe. As a matter of fact, the two scattering processes (6) and (8) (in which one of the two incoming gluons splits into $b\bar{b}$ pairs) should be considered simultaneously and their cross sections summed up with a subtraction of a common part in order to avoid double counting (see, e.g., Ref. [34, 41]). That is, from the sum of the 'flavour excitation' scattering (6) and the gluon-fusion mechanism (8), one has to subtract the piece due to the configurations in which the quark in the internal b-line (from the $g \to b\bar{b}$ splitting) in (8) is on-shell and collinear to the incoming gluon. One would expect that the total results for the combination of $bg \to bt\bar{t}$ and $gg \to b\bar{b}t\bar{t}$ events should be less μ-scale dependent then the rates for process (6) alone [41]. As a criteria to decide whether the additional b-jet falls inside the detectable region (thus mimicking a two-to-three body hard scattering) or not, we use the cut $p_T(b) \leq 20$ GeV on either of the bottom quarks (see eq. (10) below).

The total rates due to processes (6) and (8) with the mentioned subtraction as a function of the μ-scale are reported in the left-hand column of Table. II. From there, one can argue that the error associated with the scale dependence of reaction (6) should be below 30% or so. In fact, this is the difference between the value of the cross section, say, at $\mu = 2m_t$ and at 1 TeV. Such numbers correspond to the case of the MRRS(3) PDFs (our default in the following), though we have verified that similar rates also occur for the other three sets adopted here.

Finally, for completeness, we also have calculated the contribution from events of the type

$$gg \to b\bar{b}t\bar{t} \qquad \text{(via } g \to t\bar{t} \text{ and } g \to gg \text{ splittings)}, \tag{9}$$

[8]As this new approach effectively interpolates between the preceeding two, it is often referred to as the Variable-Flavour-Number (VFN) scheme.

in which one of the gluons splits into either $t\bar{t}$ or gg pairs, with one of the final state b's missed along the beam line. As a matter of fact, also such events contribute to the total rate for $bt\bar{t}$ production, on the same footing as the (8) ones do. The corresponding cross sections (with one of the b's having $p_T(b) \leq 20$ GeV) as a function of the μ-scale can be found in the right-hand column of Tab. II (i.e., in brackets). They amount to roughly 18% of the total rates in the nearby column.

For sake of simplicity in the numerical calculations, in the remainder of the paper we will only consider the rates of the process $bg \to bt\bar{t}$, thus ignoring for the time being its interplay with those of reactions (8) and (9).

3.2 $bg \to bt\bar{t}$ phenomenology

Contrary to the case of the Tevatron, at the LHC effects due to process (6) can be perceptible in various instances. For starting, the cross section is rather large per se, as it amounts to 8 pb. Therefore, with 10 fb^{-1} of Run 1 at the LHC, it yields some 80,000 $bt\bar{t}$ events per year. In one selects semi-(hadronic)leptonic SM decays, then the event rate is around 24,000.

It is interesting to separate the total cross section given previously into its pure QCD component (i.e., diagrams in Fig. 1a) and that involving EW interactions as well (i.e., diagrams in Fig. 1b). This is done in Fig. 2, for the LHC. In addition, to establish whether the presence of the Higgs graphs 4, 8, 12 and 16 (in Fig. 1b) has any influence on the total cross section we vary M_H in the range between 60 and 500 GeV. As one might expect such contributions to be particularly relevant near the $H \to t\bar{t}$ threshold (see diagrams 4 and 16 in Fig. 1b), we have enlarged the interval 340 GeV $\lesssim M_H \lesssim$ 360 GeV in the insert in the middle of the plot. As a matter of fact, the effect is visible in the EW contribution but imperceptible in the total cross section. Thus, Higgs diagrams are of no special concern, whichever the actual value of M_H is. This implies that no further theoretical uncertainty related to the unknown parameter M_H enters in our results.

The important feature in Fig. 2 is that the EW contribution is rather large in the total results. At the LHC and for $M_H = 150$ GeV this is around 3 pb, yielding some 30,000 events during Run 1 (which become 9,000 after implementing the semi-hadronic(leptonic) SM branching ratios of the two top quarks). This is around 40% of the total rate of process (6). If a fourth generation down-type flavour d_4 of mass $m_{d_4} \approx 175$ GeV is instead produced, these rates change dramatically. As previously mentioned, this is mainly due to the absence of the dominant EW diagrams 1 and 5 in Fig. 1b. However, also the different EW couplings between neutral gauge bosons (i.e., γ and Z) are responsible for differences. Tab. III shows the total cross section (pure QCD graphs plus the EW ones) for events of the type $bg \to bd_4\bar{d}_4$ against that of $bt\bar{t}$, for five values of m_{d_4} (conservatively compatible with the latest measurements of m_t). One can see that the rates are very different. Indeed, those for $bd_4\bar{d}_4$ production practically coincide with the QCD contribution of process (6) only (compare the rates in Tab. III with those in Fig. 2, when $m_t = 175$ GeV). This pattern remains unchanged for all masses considered.

Clearly, if one can isolate top-antitop events compatible with an additional b-quark in the final state, then it could be possible to search for deviations such as those revealed in Tab. III. This could be achieved in the semi-hadronic(leptonic) top decay channel by requiring two b-tags and one high p_T lepton and by reconstructing the resonant fermion mass via a three-jet system. The requirement of two vertex tags imposes an additional reduction of the detected rates. By assuming an efficiency of 60% per fiducial b-jet [44, 45], the overall one to tag two of these would then be 36%. Of the original $bt\bar{t}$ events, some 8,000+3,000 would survive during Run 1, further reduced by a factor of 9 after the following detector acceptances (on two b-jets)[9]:

$$
\begin{aligned}
|\eta(b)| < 2, \qquad & p_T(b) > 20 \text{ GeV}, \\
|\eta(\ell)| < 2.5, \qquad & p_T(\ell) > 10(20) \text{ GeV}, \\
|\eta(j)| < 4, \qquad & p_T(j) > 20 \text{ GeV}, \\
& \not{p}_T > 20 \text{ GeV}.
\end{aligned} \tag{10}
$$

The final numbers are approximately 880 and 330 for the final rates from the diagrams in Fig. 1a–b, respectively. This means that roughly 1200 events are expect within the SM from $bt\bar{t}$ production in the detection channel $bb\ell jjj$, where $\ell = e, \mu$ and j is a jet. Because of the dominance of diagrams involving two $W^{\pm}tb$ couplings in the EW component of $bt\bar{t}$ events, several hundred of $bt\bar{t}$ events will show a $|V_{tb}|^4$ dependence, which could possibly be exploited in experimental analyses to furnish an independent new measurement of the CKM matrix element. A fourth generation d-type quark d_4 with mass similar to that of the top would only produce the equivalent of the QCD component of $bt\bar{t}$, that is, 38% less events. Finally, we have verified that no intrinsic difference exists in the kinematics of the QCD and EW components in the spectra of the lepton and jets which could be profitably exploited to separate these two parts of the cross section.

3.3 Double- and single-top phenomenology

The numbers in Tab. I and Fig. 2 certainly compare rather poorly to the total rates of both double- and single-top events. In fact, the cross section for process (6) amounts to 1% of the former and 2% of the latter.

In the first case, this clearly implies that effects due to events (6) can hardly be disentangled in $t\bar{t}$ phenomenology. Indeed, one should recall that the total cross section for pair production of top quarks is made up by the two components (1)–(2) only, each of these yielding the same signature and each of these with rates much larger than those of (6). Of the 800 pb at the LHC, 730 pb come from gg- and 70 from $q\bar{q}$-fusion [6]. However, if particular kinematic configurations are selected to reduce the leading order $t\bar{t}$ rates (e.g., to disentangle some New Physics or when studying the mentioned radiative and/or three-body top decays), then $bt\bar{t}$ events could become important.

Fig. 3 (left-hand side) plots the invariant mass distributions of the system $t\bar{t}X$ for events of the type (1)–(2) and (6). From there it is clear that if one looks for inclusive signals (i.e., X represents any additional particle in the final state) and studies the total invariant mass of the final state, then a 'resonance' (dashed curve) should appear some 180 GeV above the $t\bar{t}$ threshold at $2m_t$. Furthermore, note that also the peak in the $M_{t\bar{t}}$ spectrum produced by events of the type (6) (dotted line) is shifted by several GeV (upwards) with respect to that due to $q\bar{q}$- and gg-fusion (solid line).

[9]In parentheses is the p_T threshold for charged leptons used as trigger.

The cosine of the polar angle of the (anti)lepton from the two top decays (signal of a possible contamination of $V+A$ coupling in the $W^{\pm}tb$ vertex) in $bt\bar{t}$ samples is significantly different from that originated by processes (1)–(2), as can be appreciated in right-hand side of Fig. 3. As the coefficient of a possible $V+A$ chirality violating current could well be at the level of few percent compared to that of the $V-A$ term, it is important to recognise and subtract the contribution of $bt\bar{t}$ events from the experimental sample.

If one compares the rates due to process (6) with the yield of each of the subprocesses contributing to single-top production, one discovers that the 400 pb cross section (including all charged conjugated processes) for $pp \to tX$ (X does not include here a second t-quark) is built up in the following way [6]: $pp \to tqX$ yields 253 pb, $pp \to tW^{\pm}X$ produces 128 pb whereas $pp \to tbX$ gives 19 pb [6]. Therefore, the rates of process (6) are similar to those for single-top production in association with a bottom quark.

The latter process has a particular relevance in single-top phenomenology. In fact, there are three parton subprocesses yielding final states of the type, say, $t\bar{b}X$ (i.e., for top-antibottom pairs). Namely, (i) $q'\bar{q} \to t\bar{b}$; (ii) $q'g \to t\bar{b}q$; (iii) $q'\bar{q} \to t\bar{b}g$ (see Ref. [9])[10]. Among these, the 'ideal' one to be exploited in phenomenological studies would be $q'\bar{q} \to t\bar{b}$ [46]. This is because the corresponding cross section can be reliably calculated, for several reasons. First, the light (anti)quark distribution functions inside the proton are evaluated at moderate values of x where they are well known. Second, the QCD corrections to this process can be calculated easily (they plug into a pure EW process) up to the order $\mathcal{O}(\alpha_s^2)$. Those from the initial state are taken into account by simply constraining the quark-antiquark flux via a measurement of the rates for $q'\bar{q} \to \ell\nu_\ell$. Those from the final state can be incorporated without ambiguities as there are no collinear and soft singularities. As a matter of fact, the two radiations do not interfere until the $\mathcal{O}(\alpha_s^2)$ order. Furthermore, the kinematics is that of a two-to-two body process, whereas cases (ii) and (iii) involve an additional light jet in the final state, thus case (i) is easier to reconstruct experimentally. More in general, the process $q'\bar{q} \to t\bar{b}$ can boast the same advantages with respect to any of the other single-top production channels. For one or more of the following reasons. Firstly, the latter always involve either a gluon, a b or both in the initial state[11]. Secondly, they proceed via QCD interactions. Thirdly, singularities can occur at higher orders in α_s. Therefore, in the first case, they suffer from larger uncertainties due the rather unknown corresponding PDFs and, in the second and third cases, the inclusion of higher order QCD effects is in general much less trivial[12].

The cross section for $q'\bar{q} \to t\bar{b}$ at the LHC, before any acceptance cuts, is around 9 pb [46] (including C.C. processes), almost the same as that of process (6), thus the latter must be considered as possible dangerous source of background events. To establish its relevance in this context, we proceed as follows. First, we calculate the cross section of events of the type (6) in which the additional b-quark in the final state escapes detection. In this case, the final state recorded in the detectors is $t\bar{t}$. Then, we select semi-leptonic(hadronic)

[10]Note that in case (ii) only graphs with gluons coupled to light quarks are considered, as those involving $g \to b\bar{b}$ and $g \to t\bar{t}$ splitting form a separate gauge invariant set and need to be considered apart, because of the definition of the b-sea quarks in the partonic distributions (see discussion in Ref. [9]).

[11]The only exception is $q\bar{q} \to tW^-\bar{b}$, which is however two orders of magnitude smaller [9] and with a more complicated final state.

[12]This is also true for the simple two-to-two EW process $q'b \to qt$, where collinear and infrared divergences along the massless $q'q$ line spoil the advantages from the factorisation of the strong corrections at the order $\mathcal{O}(\alpha_s)$.

decays $t\bar{t} \to b\bar{b}W^+W^- \to b\bar{b}\ell\nu_\ell jj$, where $\ell = e, \mu$ and j represents a light quark jet, originated by the fragmentation of a u-, d-, s- or c-quark. To appreciate the kinematics of the additional final state b-quark in reaction (6) one can refer to Fig. 5, where its distributions in transverse momentum p_T and pseudorapidity η are plotted, along with those of all the other final state particles, as they would appear at the LHC[13]. We introduce here a distinction between the three b's in the final state of (6), that we will maintain in the following. This because they have different kinematic behaviours. We call 'prompt b' that produced in association with the $t\bar{t}$ pair, 'direct b' that coming from the decay of the top in Fig. 1a–b and 'indirect b' the remaining one from the antitop[14]. Such a distinction has phenomenological relevance for the 'prompt b' for the key rôle that it plays in the determination of the observed rates of process (6), whereas in the other two cases it has been made for sake of illustration only. In the first case, one can appreciate the striking behaviour of the parton in Fig. 5, as this tends to be emitted almost exclusively along the beam pipe, with $p_T < 20$ GeV and $|\eta| > 4$. For the other two b's, one should recognise that, although the production dynamics of the 'direct b' and the 'indirect b' is different (at least in the diagrams of Fig. 1b, not in those of Fig. 1a) and this can be spotted in the left hand side plots of Fig. 5 (and 4 too), the differences cannot possibly be disentangled experimentally. We shall now proceed by performing the same selection procedure outlined in Ref. [46] and will compare the yield of process (6) with those presented there.

The acceptance cuts implemented to simulate the detectors are those already mentioned in eq. (10), supplemented by the further requirements of separation (in general, on the 'direct' and 'indirect' b's):

$$|\Delta R_{bb}| > 0.7, \qquad\qquad |\Delta R_{b\ell}| > 0.7. \tag{11}$$

Note that in applying cuts (10)–(11) to process (6) in the context of single-top phenomenology one only has four jets in the selected final state (two b-jets and two light flavour ones), as one of the three produced b-quarks (in general, the 'prompt' b) is assumed to be lost along the beam pipe. The cross section of $bg \to bt\bar{t}$ events after the above acceptance cuts is approximately 1600 fb. After implementing the branching ratio 2/9 for electronic and/or muonic decays of the tagged $W^\pm$ one gets $\sigma \approx 360$ fb, thus 3,600 events during Run 1 at the LHC (with ten inverse femtobarns). The rate obtained for process $q'\bar{q} \to t\bar{b}$ in Ref. [46] after the same requirements and in the same detection channel is (reading from Tab. 1 in that paper) 580 fb (including charge conjugation). The signal is thus a factor of approximately 1.6 above the background from process (6). The application of the cut $M_{b\bar{b}} > 110$ GeV (see again Ref. [46]) imposes a factor of two of reduction on $bt\bar{t}$ events. Finally, we obtain an additional drastic rejection against the latter, because of the additional $W^\pm$ in the final state. In fact, as can be appreciated in Fig. 5, any additional

[13]Note that we also have plotted (in Fig. 4) the same rates for the Tevatron, although we have already assessed that they are of no relevance at such a collider. We have done so simply to show quantitatively that the percentage of events (6) with the first b-quark produced escaping detection because of the finite coverage in p_T and η is much higher at larger energies: compare the solid curves in the two plots on the left hand side of Figs. 4 and 5. In contrast, the detector requirements on the other particles in the final state are equally effective at both Tevatron and LHC energies (dashed and dotted lines in the left windows and all curves in the right ones).

[14]The labelling works the other way around for the last two b's if $\bar{b}g$ induced diagrams are considered. Note that in the caption of Figs. 4–5 we have applied the distinction between 'direct' and 'indirect' also top the (anti)top decay products.

light flavour jet j in reaction (6) falls inside the acceptance region defined by $p_T(j) > 20$ GeV and $|\eta(j)| < 4$ [46]. We estimate that the final cross section for $bt\bar{t}$ events, after light flavour jet rejection and after including vertex tagging efficiency would be of a few femtobarns, that is one order of magnitude smaller than the signal and two orders smaller than the background rates obtained from $W^\pm b\bar{b}$, $W^\pm jj$, $W^\pm Z$, $t\bar{b}j$ and $t\bar{t}$ background events [46]. Therefore, also in single-top SM phenomenology events of the type (6) are well under control, though they represent a sizable correction (of several percent) to the $q'\bar{q} \to t\bar{b}$ signal, which should be considered when searching for New Physics.

4. Summary and conclusions

In this paper we have studied top-antitop production in association with an additional b-quark at the Tevatron and the LHC. The interest in this process for top studies at hadronic colliders comes from the fact that the b-quark is in most cases at low transverse momentum and large rapidity, so it tends to escape the acceptance region of the detectors. Therefore, such events enter naturally in the candidate $t\bar{t}$ sample and should then be considered if one wants to carry out detailed studies of top quark properties.

We have shown that at the Tevatron the total cross section for such events is negligibly small, around 2–3 fb for the upgraded Fermilab $p\bar{p}$ collider with $\sqrt{s}_{p\bar{p}} = 2$ TeV. In contrast, at the CERN accelerator the corresponding number is 8 pb. This should yield about 80,000 events after Run 1 for an accumulated luminosity of 10 inverse femtobarns. Though such a number is certainly affected by a large indetermination due to the b-structure functions, we believed it reasonably large anyway so to consider in detail the relevance of $bt\bar{t}$ events at the LHC, both as a background to double- and single-top events and as a signal on its own. As for the error associated to the parton density of b-quarks, we have given an estimate of its *lower limit*, of about 10%, by comparing the total rates as obtained from four very recent sets of parton distributions, all implementing the heavy quark dynamics in the context of the newly developed Variable-Flavour-Number (factorisation) scheme. Furthermore, we have established a 30% uncertainty of the total rates, depending on the choice of the factorisation scale μ, which was varied between twice the top mass and the TeV scale. (Indeed, to minimise the impact of the two mentioned errors, we have neglected the absolute normalisation of the relevant differential rates.)

In the case of double-top physics, it has been shown that the total rate of $bt\bar{t}$ events is small, as it represents a correction of 1% only to the QCD signal via $q\bar{q}, gg \to t\bar{t}$. However, this effect could be above the experimental accuracy and further enhanced by dedicated selection procedures (especially in order to disentangle possible effects due to New Physics), so that it should be considered when proceeding to MC simulations. In particular, the kinematics of the top quarks in $bt\bar{t}$ events is very different from that of the leading $t\bar{t}$ production: for example, in the $M_{t\bar{t}X}$ invariant mass, where X represents any additional particle in the final state. In fact, the three-jet mass distribution $M_{t\bar{t}b}$ is much broader then the $M_{t\bar{t}}$ one and the peak of the resonance is shifted by +180 GeV whereas the two-jet one $M_{t\bar{t}}$ is indeed similar to that of $t\bar{t}$ events but the shape of the threshold resonance is distorted. Finally, the spectra in the polar angle of the decay leptons differ significantly from those produced by ordinary $t\bar{t}$ events.

In the case of single-top physics, it has been demonstrated that the $bt\bar{t}$ production rates are similar to the yield of the process $q'\bar{q} \to t\bar{b}$, which has been advocated as the best channel to probe the $W^{\pm}tb$ vertex of the underlying theory. Once an appropriate selection strategy of $t\bar{b}$ events is adopted, the $bt\bar{t}$ ones are however greatly reduced. Nonetheless, the latter should anyway be included in the experimental simulations aiming to measure the Cabibbo-Kobayashi-Maskawa matrix element $|V_{tb}|$ and to test the vector/axial structure of the top-bottom-$W^{\pm}$ coupling, as violations of the SM dynamics could well be at the same level and show the same kinematic features as those due to the $bt\bar{t}$ corrections.

As for signal on its own, events of the type $bg \to bt\bar{t}$ have been proved to be extremely sensitive to the possible presence of a fourth generation of quarks, involving a down-type fermion d_4 with mass similar to that of the top, which could then mimic the latter. This is due to the fact that the EW contribution (dependent on the flavour of the produced fermion) is almost 40% of the total $bt\bar{t}$ rates and almost coincides with diagrams involving off-shell $W^{\pm}$-currents, which are naturally absent in case of $bd_4\bar{d}_4$ production. Thus, if the measured cross section suffered from a large depletion, this would indicate that the heavy particle detected recently at the Tevatron is indeed a new flavour of the theory. Conversely, about 40% of the total $bt\bar{t}$ Standard Model cross section shows a $|V_{tb}|^4$ dependence, so that top-antitop events accompanied by an additional b-quark could be exploited to obtain a new independent measurement of this crucial quantity.

5. Acknowledgements

We are grateful to the UK PPARC for financial support.

References

[1] R.K. Ellis, Phys. Lett. **B259**, 492 (1991);
E. Laenen, J. Smith and W.L. van Neerven, Phys. Lett. **B321**, 254 (1994);
E. Berger and H. Contopanagos, Phys. Lett. **B361**, 115 (1995); Phys. Rev. **D54**, 3085 (1996);
S. Catani, M. Mangano, P. Nason and L. Trentadue, Phys. Lett. **B378**, 329 (1996);
N. Kidonakis and J. Smith, Phys. Rev. **D51**, 6092 (1995);
S. Frixione, M. Mangano, P. Nason and G. Ridolfi, Phys. Lett. **B351**, 555 (1995).

[2] CDF Collaboration, Phys. Rev. Lett. **74**, 2626 (1995);
D0 Collaboration, Phys. Rev. Lett. **74**, 2632 (1995).

[3] R. Raja, presented at the *XXXII Rencontres de Moriond on Electroweak Interactions and Unified Theories*, Les Arcs, Savoie, France, March 15–22, 1997;
M. Cobal, presented at the *Fifth Topical Seminar on the Irresistible Rise of the Standard Model*, San Miniato, Tuscany, Italy, April 21–25, 1997.

[4] A. Blondel, plenary talk given at the International Conference on High Energy Physics, Warsaw, 1996.

[5] S. Dawson, Nucl. Phys. **B249**, 42 (1985);
S.S.D. Willenbrock and D.A. Dicus, Phys. Rev. **D34**, 155 (1986);

S. Dawson and S.S.D. Willenbrock, Nucl. Phys. **B284**, 449 (1987);
C.-P. Yuan, Phys. Rev. **D41**, 42 (1990);
T. Moers, R. Priem, D. Rein and H. Reitler, in Proceedings of the ECFA Large Hadron Collider Workshop: Physics and Instrumentation, Aachen, Germany, 1990, edited by G. Jarlskog and D. Rein (CERN, 1990);
G.V. Jikia and S.R. Slabospitsky, Phys. Lett **B295**, 136 (1992);
R.K. Ellis and S. Parke, Phys. Rev. **D46**, 3785 (1992);
G. Bordes and B. van Eijk, Z. Phys. **C57**, 81 (1993);
D.O. Carlson and C.-P. Yuan, Phys. Lett. **B306**, 386 (1993);
G. Bordes and B. van Eijk, Nucl. Phys. **B435**, 23 (1995);
F. Anselmo, G. Bordes and B. van Eijk, Phys. Rev. **D45**, 2312 (1992);
D.O. Carlson and C.-P. Yuan, to appear in Proceedings of the Workshop on Physics of the Top Quark, Ames, Iowa, (May 1995), [hep-ph/9509208];
A.P. Heinson, A.S. Belyaev and E.E. Boos, to appear in Proceedings of the Workshop on Physics of the Top Quark, Ames, Iowa, (May 1995), [hep-ph/9509274];
S. Cortese and R. Petronzio, Phys. Lett. **B253**, 494 (1991);
T. Stelzer and S.S.D. Willenbrock, Phys. Lett. **B357**, 125 (1995);
R. Pittau, Phys. Lett. **B386**, 397 (1996);
M. Smith and S.S.D. Willenbrock, Phys. Rev. **D54**, 6696 (1996);
D. Atwood, S. Bar-Shalom, G. Eilam and A. Soni, Phys. Rev. **D54**, 5412 (1996);
C.S. Li, R.J. Oakes and J.M. Yang, Phys. Rev. **D55**, 1672 (1997); Phys. Rev. **D55**, 5780 (1997);
A.P. Heinson, A.S. Belyaev and E.E. Boos, Phys. Rev. **D56**, 3114 (1997);
G.A. Ladinsky and C.-P. Yuan, Phys. Rev. **D43**, 789 (1991);
T. Stelzer, Z. Sullivan and S.S.D. Willenbrock, [hep-ph/9705398].

[6] See, e.g.:
A.P. Heinson, Talk given at the XXXIst Rencontres de Moriond, QCD and High Energy Hadronic Interactions, Les Arcs, Savoie, France, 23rd-30th March 1996, Fermilab-Conf-96/116-E, May 1996, [hep-ex/9605010].

[7] D.O. Carlson, E. Malkawi and C.-P. Yuan, Phys. Lett. **B337**, 145 (1994);
E. Malkawi and C.-P. Yuan, Phys. Rev. **D50**, 4462 (1994);
C.-P. Yuan, Mod. Phys. Lett. **A10**, 627 (1995);
T.G. Rizzo, Phys. Rev. **D53**, 6218 (1996);
G. Mahlon and S. Parke, Phys. Rev. **D55**, 7249 (1997).

[8] See, e.g.:
Particle Data Group, Phys. Rev. **D54**, 1 (1996) (and references therein).

[9] A.P. Heinson, A.S. Belyaev and E.E. Boos, in Ref. [5].

[10] See, e.g.:
P. Tipton, plenary talk given at the International Conference on High Energy Physics, Warsaw, 1996;
S.S.D. Willenbrock, plenary talk given at the International Conference on High Energy Physics, Warsaw, 1996.

[11] F.I. Olness and R.J. Scalise, preprint CTEQ-708, SMU-HEP-9709, July 1997, [hep-ph/9707459].

[12] L.H. Orr, T. Stelzer and W.J. Stirling, talk given at the 1996 Annual Divisional Meeting (DPF 96) of the Division of Particles and Fields of the American Physical Society, Minneapolis, MN, 10-15 August 1996, preprint UR-1477, ER-40685-893, C96-08-10, September 1996, [hep-ph/9609354]; Phys. Rev. **D56**, 446 (1997); Phys. Lett. **B354**, 442 (1995); Phys. Rev. **D52**, 124 (1995);
V.A. Khoze, L.H. Orr and W.J. Stirling, Nucl. Phys. **B378**, 413 (1992);
V.A. Khoze, J. Ohnemus and W.J. Stirling, Phys. Rev. **D49**, 1237 (1994).

[13] G. Mahlon and S. Parke, Phys. Lett. **B347**, 394 (1995).

[14] See, e.g.:
R.D. Peccei, S. Peris and X. Zhang, Nucl. Phys. **B349**, 305 (1991).

[15] For a review paper see, e.g.:
K. Lane, preprint BUHEP-96-8, May 1996, [hep-ph/9605257] (and references therein).

[16] C.T. Hill and S.J. Parke, Phys. Rev. **D49**, 4454 (1994);
S. Parke, to appear in Proceedings of the Symposium on Heavy Flavour and Electroweak Theory, Beijing, China, August 1995, [hep-ph/9511468] (and references therein).

[17] J. Reid, G. Tupper, G.W. Li and M.A. Samuel, Z. Phys. **C51**, 395 (1991);
C.-S. Li, B.-Q. Hu and J.M. Yang, Phys. Rev. **D51**, 4971 (1995); Erratum, ibidem **D53**, 5325 (1996).

[18] V. Barger and R.J.N. Phillips, Phys. Rev. **D40**, 2875 (1989) (and references therein).

[19] S. Mrenna and C.-P. Yuan, Phys. Lett. **B367**, 188 (1996).

[20] N.G. Deshpande, B. Margolis and H.D. Trottier, Phys. Rev. **D45**, 178 (1992);
D. Atwood, A. Aeppli and A. Soni, Phys. Rev. Lett. **69**, 2754 (1992);
D. Atwood, A. Kagan and T.G. Rizzo, Phys. Rev. **D52**, 6264 (1995);
C.-S. Huang and T.-J. Li, Z. Phys. **C68**, 319 (1995);
K. Cheung, Phys. Rev. **D53**, 3604 (1996);
J. Berger, A. Blotz, H.-C. Kim and K. Goeke, Phys. Rev. **D54**, 3598 (1996);
T. Tait and C.-P. Yuan, Phys. Rev. **D55**, 7300 (1997).

[21] C.T. Hill, Phys. Lett. **B266**, 419 (1991);
E. Eichten and K. Lane, Phys. Lett. **B327**, 129 (1994);
L.L. Smith, P. Jain and D.W. McKay, to appear in Proceedings of the 9th Annual American Physical Society Division of Particles and Fields Meeting, Minneapolis, MN, August 1996, [hep-ph/9608328];
A. Datta and X. Zhang, Phys. Rev. **D55**, 2530 (1997);
E.H. Simmons, Phys. Rev. **D55**, 5494 (1997);
G. Lu., Y. Cao, J. Huang, J. Zhang and Z. Xiao, preprint HNU-TH-97-01, January 1997, [hep-ph/9701406];
A. Datta, J.-M. Yang, B.-L. Young and X. Zhang, Phys. Rev. **D56**, 3107 (1997).

[22] M. Ježabek and J.H. Kühn, Phys. Lett. **B329**, 317 (1994);
G. Kane, C.-P. Yuan and G. Ladinsky, Phys. Rev. **D45**, 124 (1992);
V. Barger, J. Ohnemus and R.J.N. Phillips, Int. J. Mod. Phys. **A4**, 617 (1989);
D.O. Carlson and C.-P. Yuan, Phys. Lett. **B306**, 386 (1993);
T. Stelzer and S.S.D. Willenbrock, Phys. Lett. **B374**, 169 (1996);
G. Mahlon and S. Parke, Phys. Rev. **D53**, 4886 (1996);
A. Brandenburg, Phys. Lett. **B388**, 626 (1996).

[23] T. Stelzer and W.F. Long, Comp. Phys. Comm. **81**, 357 (1994).

[24] H. Murayama, I. Watanabe and K. Hagiwara, HELAS: HELicity Amplitude Subroutines for Feynman Diagram Evaluations, *KEK Report* 91-11, January 1992.

[25] C. Becchi, A. Rouet and R. Stora, Ann. Phys. **98**, 287 (1976);
G.J. Gounaris, R. Kogerler and H. Neufeld, Phys. Rev. **D34**, 3257 (1986).

[26] G.P. Lepage, Jour. Comp. Phys. **27**, 192 (1978).

[27] V.N. Gribov and L.N. Lipatov, Sov. J. Nucl. Phys. **15**, 438 (1972); ibidem **15**, 675 (1972);
Yu.L. Dokshitzer, Sov. Phys. JETP **46**, 641 (1977);
G. Altarelli and G. Parisi, Nucl. Phys. **B126**, 298 (1977).

[28] A.D. Martin, R.G. Roberts and W.J. Stirling, Phys. Rev. **D50**, 6734 (1994).

[29] A.D. Martin, R.G. Roberts and W.J. Stirling, Phys. Lett. **B354**, 155 (1995).

[30] A.D. Martin, R.G. Roberts and W.J. Stirling, Phys. Lett. **B387**, 419 (1996).

[31] A.D. Martin, R.G. Roberts, M.G. Ryskin and W.J. Stirling, preprint DTP/96/102, December 1996, [hep-ph/9612449].

[32] H.L. Lai, J. Botts, J. Huston, J.G. Morfin, J.F. Owens, J. Qiu, W.K. Tung and H. Weerts, Phys. Rev. **D51**, 4763 (1995).

[33] H.L. Lai, J. Huston, S. Kuhlmann, F. Olness, J.F. Owens, D. Soper, W.K. Tung and H. Weerts, Phys. Rev. **D55**, 1280 (1997).

[34] H.L. Lai and W.K. Tung, Z. Phys. **C74**, 463 (1997).

[35] W.J. Marciano, Phys. Rev. **D29**, 580 (1984).

[36] J.P. Martin, talk given at the International Conference on High Energy Physics, Warsaw, 1996.

[37] The LEP Electroweak Working Group and the SLD Heavy Flavor Group, preprint LEPEWWG/96-02, ALEPH 96-107 PHYSIC 96-98, DELPHI 96-121 PHYS 631, L3 Note 1975, OPAL Technical Note TN 399, SLD Physics Note 52, 30 July 1996.

[38] A. Ballestrero, E. Maina and M. Pizzio, Phys. Lett. **B387**, 411 (1996).

[39] M. Gluck, E. Reya and A. Vogt, Z. Phys. **C67**, 433 (1995).

[40] M. Gluck, E. Hoffmann and E. Reya, Z. Phys. **C13**, 119 (1982);
S. Kretzer, E. Reya and M. Stratmann, Phys. Lett. **B348**, 628 (1995).

[41] M.A.G. Aivazis, F.I. Olness and W.K. Tung, Phys. Rev. **D50**, 3085 (1994); Phys. Rev. **D50**, 3102 (1994).

[42] M. Buza, Y. Matiounine, J. Smith and W.L. van Neerven, preprint NIKHEF-96-027, ITP-SB-96-66, DESY-96-258, INLO-PUB-22-96, December 1996, [hep-ph/9612398]; preprint NIKHEF-97-026, ITP-SB-97-35, DESY-97-124, INLO-PUB-6-97, July 1997, [hep-ph/9707263].

[43] V. Barone and M. Genovese, *Phys. Lett.* **B379**, 233 (1996);
V. Barone, U. d'Alesio and M. Genovese, [hep-ph/9610211].

[44] CMS Technical Proposal, CERN/LHC/94-43 LHCC/P1 (December 1994).

[45] ATLAS Technical Proposal, CERN/LHC/94-43 LHCC/P2 (December 1994).

[46] T. Stelzer and S. Willenbrock, in Ref. [5].

Table Captions

[I] Total cross sections (QCD and EW summed) for process (6) at the LHC for four different sets of structure functions. Errors are as given by VEGAS.

[II] Total cross sections (QCD and EW summed) for process (6) at the LHC for four different choices of the scale parameter. In parentheses are the corresponding rates for process (9). The MRRS(3) structure functions have been used. Errors are as given by VEGAS.

[III] Total cross sections (QCD and EW summed) for processes $bg \to bd_4\bar{d}_4$ (see the text) and (6) at the LHC for five different masses m_t/m_{d_4}. The MRRS(3) structure functions have been used. Errors are as given by VEGAS.

Figure Captions

[1] Lowest order Feynman diagrams describing process (6): (**a**) the $\mathcal{O}(\alpha_s^3)$ contribution; (**b**) the $\mathcal{O}(\alpha_s \alpha_{em}^2)$ contribution. The package MadGraph [23] has been used to produce the PostScript file. In (**b**) 'A' represents a photon and the dashed line identifies the SM Higgs boson.

[2] Cross sections for process (6) at the LHC as a function of the Higgs mass. The MRRS(3) structure functions have been used. Solid line: process (6), $\mathcal{O}(\alpha_s^3) + \mathcal{O}(\alpha_s \alpha_{em}^2)$ rates. Dashed line: process (6), $\mathcal{O}(\alpha_s \alpha_{em}^2)$ rates.

[3] Left window: differential distributions in invariant mass of the systems $t\bar{t}$ in events of the type (1)–(2) (solid line), $bt\bar{t}$ in events of the type (6) (dashed line), $t\bar{t}$ in events of the type (6) (dotted line). Right window: differential distributions in polar angle of the lepton in events of the type (1)–(2) (solid line), antilepton in events of the type (1)–(2) (dashed line), lepton in events of the type (6) (dotted line), antilepton in events of the type (6) (dash-dotted line). Normalisations are to unity.

[4] Differential distributions in transverse momentum (upper two plots) and in pseudorapidity (lower two plots) of the particles in the final state of process (6) at the Tevatron. All QCD and EW contributions have been considered. On the left hand side, spectra of the three b-quarks: 'prompt b' (solid line); 'direct b' (dashed line) and 'indirect b' (dotted line). On the right hand side, spectra of the leptons and light quark jets: 'direct leptons/jets' (solid and dotted lines) and 'indirect leptons/jets' (dashed and dot-dashed lines). Each curve is normalised to unity. The MRRS(3) structure functions have been used.

[5] Same as Fig. 4 at the LHC.

σ_{tot} (fb)	
PDFs	$\sqrt{s}_{pp} = 14$ TeV
MRRS(1)	8117 ± 25
MRRS(2)	8135 ± 26
MRRS(3)	8101 ± 24
CTEQ(4HQ)	8996 ± 23
$M_H = 150$ GeV	
no acceptance cuts	

Tab. I

σ_{tot} (fb)	
μ (GeV)	$\sqrt{s}_{pp} = 14$ TeV
$2m_t$	$10474 \pm 38(1856.3 \pm 8.6)$
400	$10030 \pm 36(1719.2 \pm 6.9)$
500	$9459 \pm 32(1505.8 \pm 6.2)$
600	$8913 \pm 30(1356.4 \pm 5.6)$
700	$8539 \pm 27(1242.3 \pm 5.1)$
800	$8258 \pm 24(1153.4 \pm 4.9)$
900	$8019 \pm 22(1082.5 \pm 4.6)$
1000	$7802 \pm 19(1010.3 \pm 4.4)$
$M_H = 150$ GeV	
no acceptance cuts	
MRRS(3)	

Tab. II

σ_{tot} (fb)		
m_{d_4}/m_t (GeV)	$bg \to bd_4\bar{d}_4$	$bg \to bt\bar{t}$
165	7112 ± 27	11303 ± 34
170	6142 ± 25	10062 ± 27
175	5319 ± 25	8101 ± 24
180	4626 ± 23	8093 ± 20
185	4029 ± 17	7305 ± 18
$M_H = 150$ GeV		
no acceptance cuts		
MRRS(3)		
$\sqrt{s_{pp}} = 14$ TeV		

Tab. III

Diagrams by MadGraph

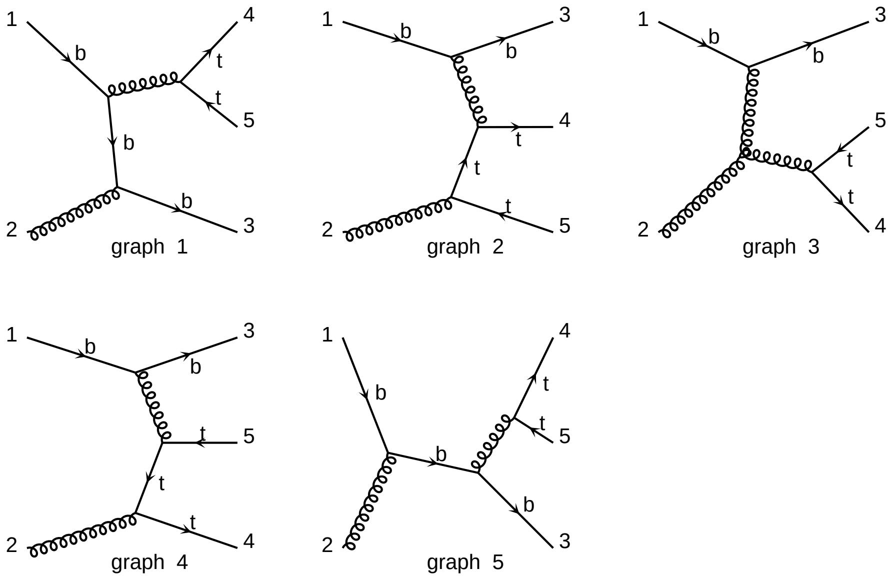

Fig. 1a

Diagrams by MadGraph

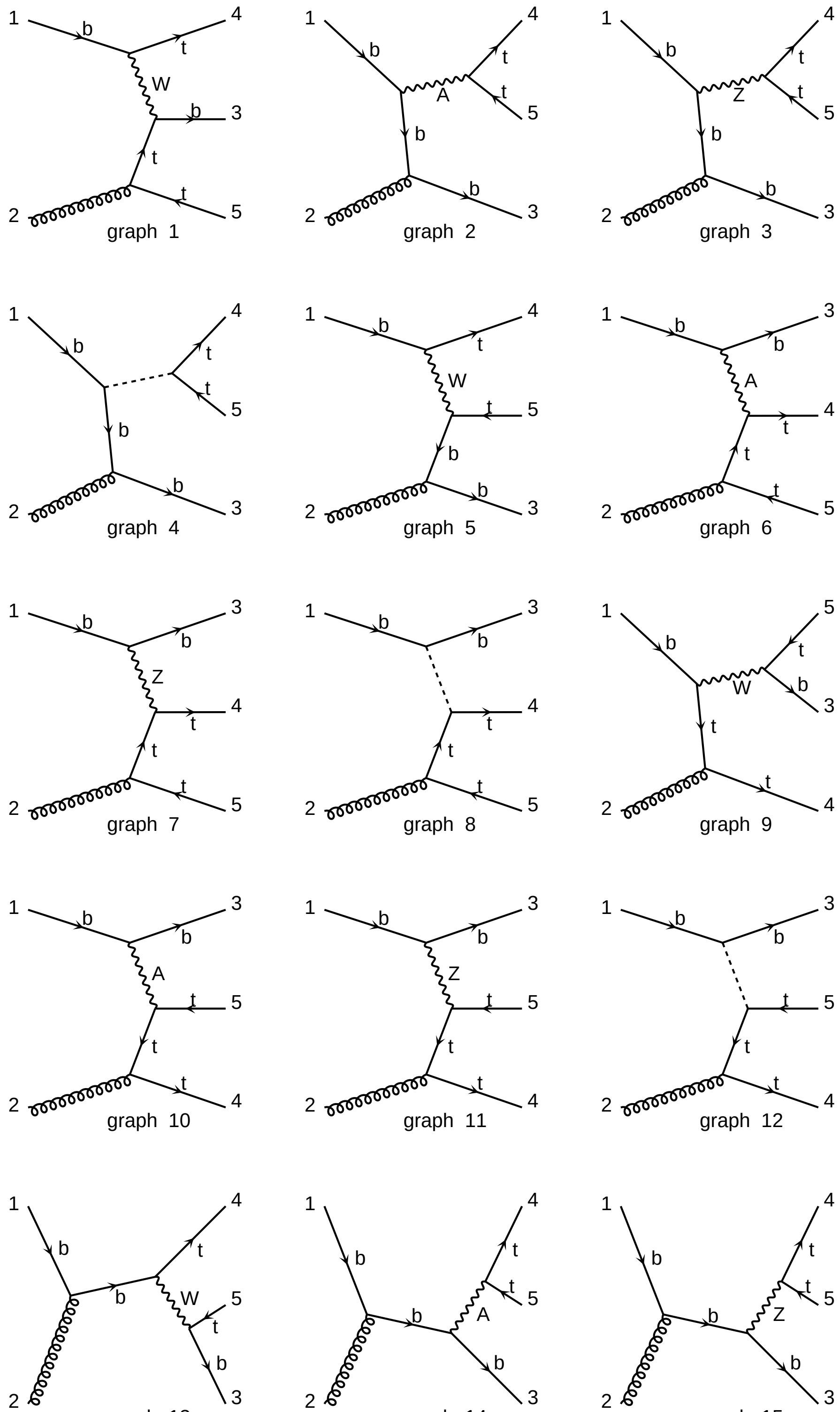

graph 1, graph 2, graph 3, graph 4, graph 5, graph 6, graph 7, graph 8, graph 9, graph 10, graph 11, graph 12, graph 13, graph 14, graph 15

Diagrams by MadGraph

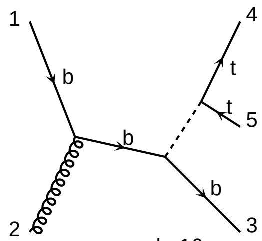

Fig. 1b

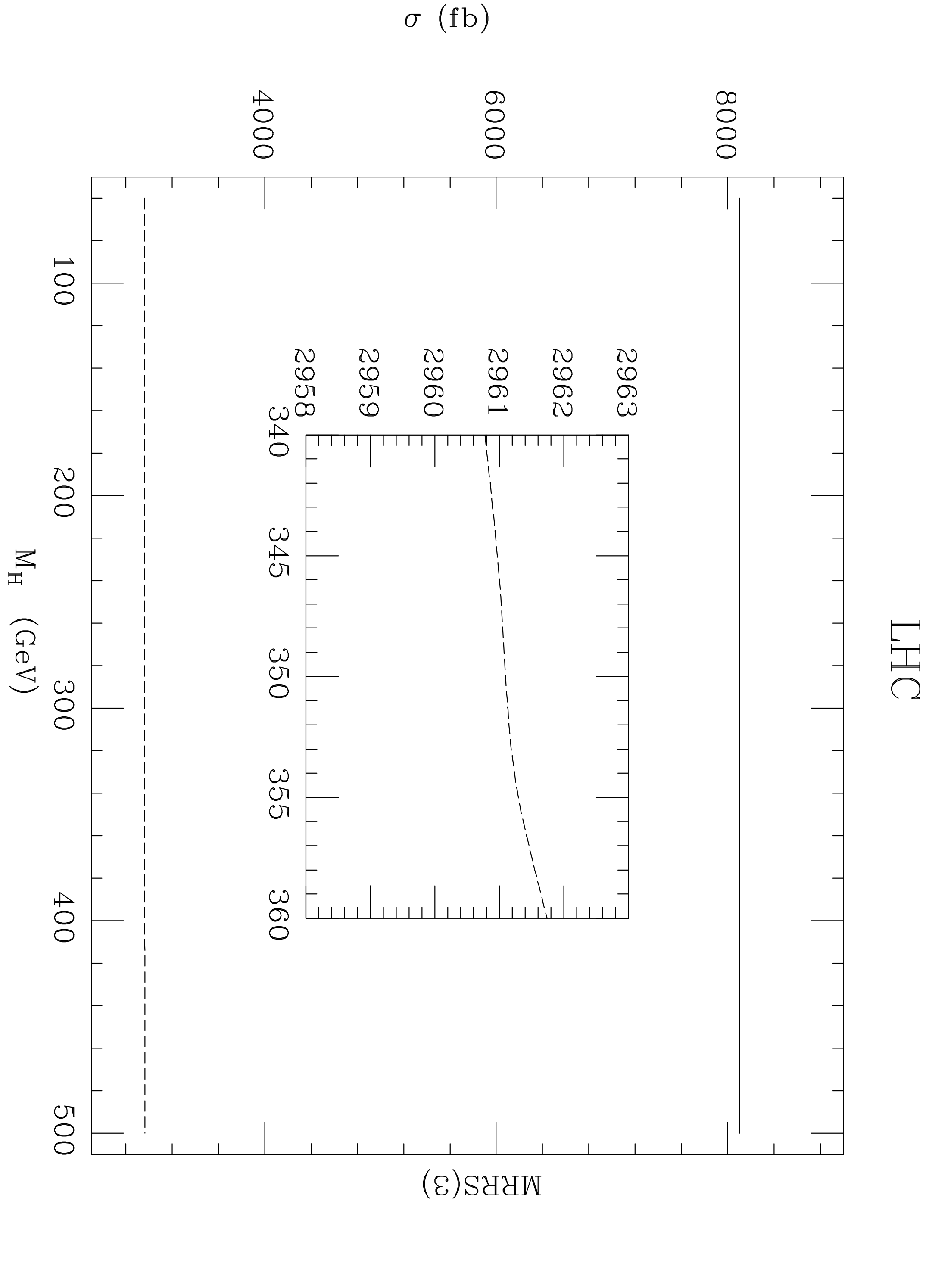

LHC
σ (fb)
4000
6000
8000
100
200
300
400
500
M_H (GeV)
2958
2959
2960
2961
2962
2963
340
345
350
355
360
MRRS(3)

Fig. 2

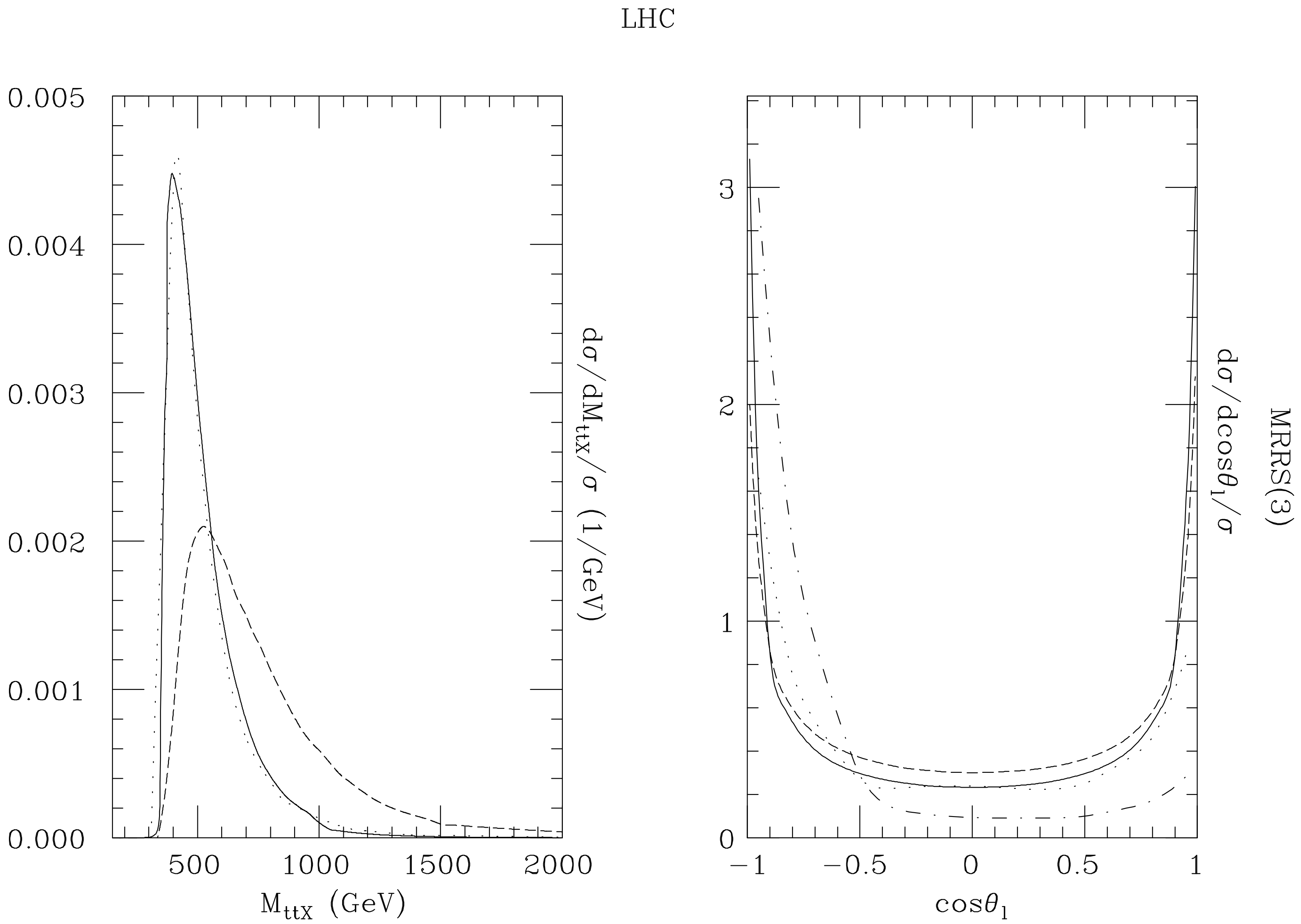
LHC
0.005
0.004
0.003
0.002
0.001
0.000
500
1000
1500
2000
M_{ttX} (GeV)
$d\sigma/dM_{ttX}/\sigma$ (1/GeV)
0
1
2
3
−1
−0.5
0
0.5
1
$\cos\theta_1$
$d\sigma/d\cos\theta_1/\sigma$
MRRS(3)

Fig. 3

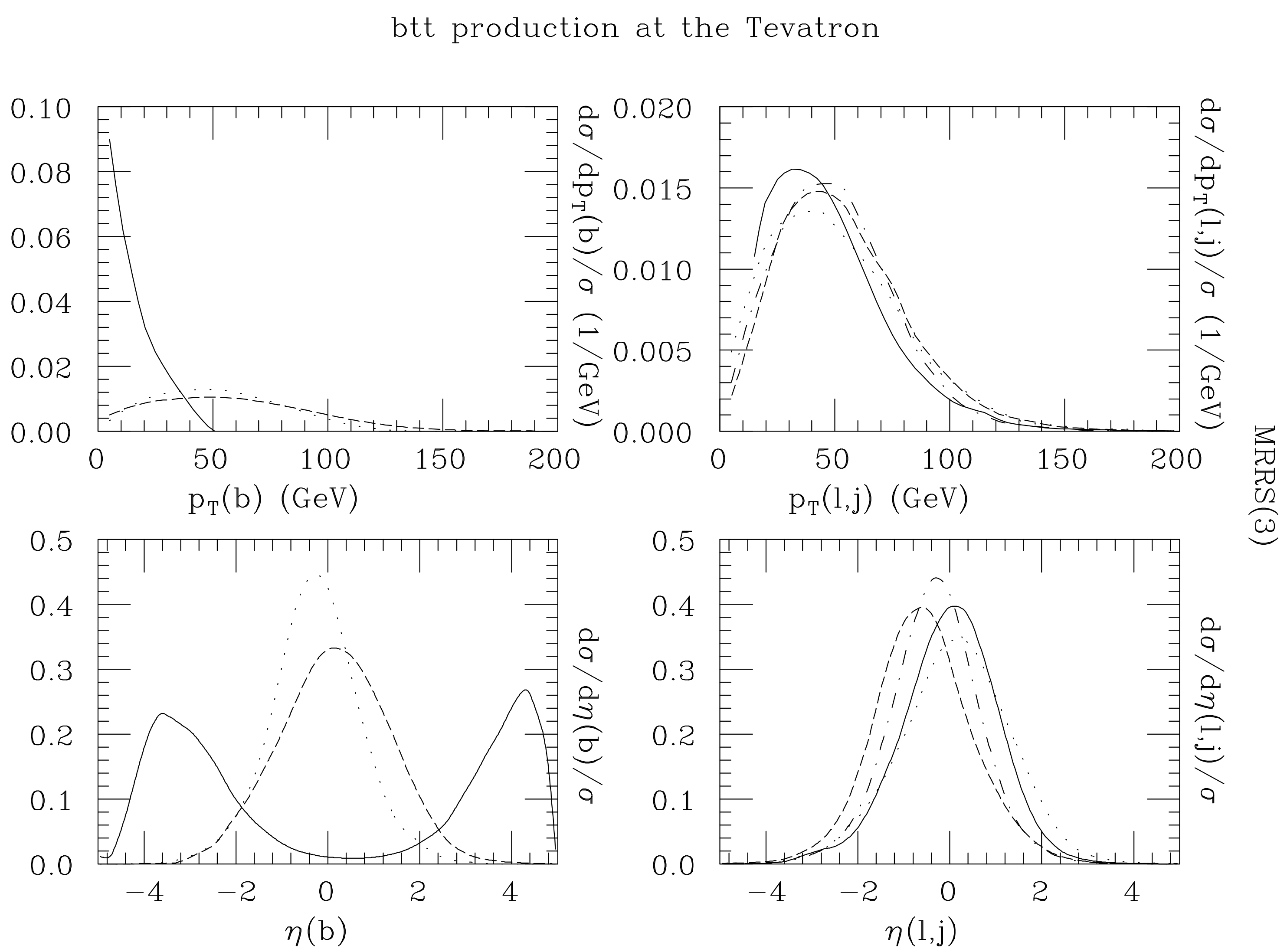
btt production at the Tevatron
$d\sigma/dp_T(b)/\sigma$ (1/GeV)
$p_T(b)$ (GeV)
$d\sigma/dp_T(l,j)/\sigma$ (1/GeV)
$p_T(l,j)$ (GeV)
$d\sigma/d\eta(b)/\sigma$
$\eta(b)$
$d\sigma/d\eta(l,j)/\sigma$
$\eta(l,j)$
MRRS(3)

Fig. 4

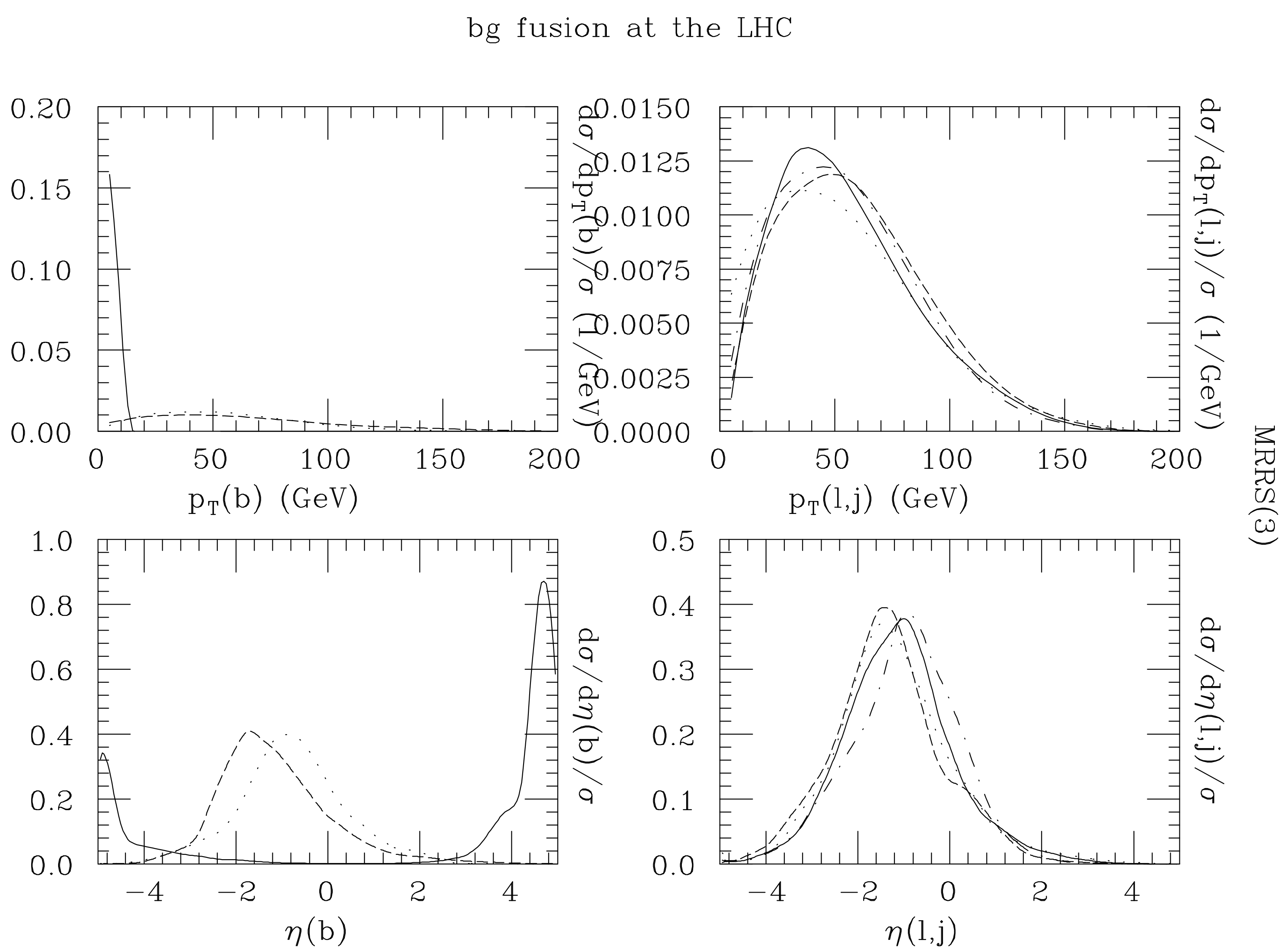
bg fusion at the LHC
0.20
0.15
0.10
0.05
0.00
0
50
100
150
200
$p_T(b)$ (GeV)
$d\sigma/dp_T(b)/\sigma$ (1/GeV)
0.0150
0.0125
0.0100
0.0075
0.0050
0.0025
0.0000
$p_T(l,j)$ (GeV)
$d\sigma/dp_T(l,j)/\sigma$ (1/GeV)
1.0
0.8
0.6
0.4
0.2
0.0
−4
−2
0
2
4
$\eta(b)$
$d\sigma/d\eta(b)/\sigma$
0.5
0.4
0.3
0.2
0.1
$\eta(l,j)$
$d\sigma/d\eta(l,j)/\sigma$
MRRS(3)

Fig. 5